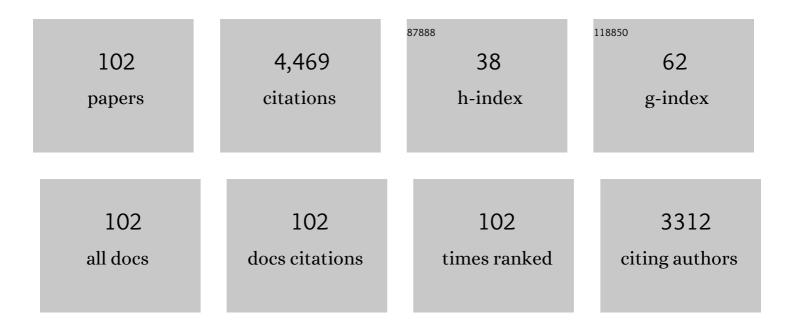
Gaohong He

List of Publications by Year in descending order

Source: https://exaly.com/author-pdf/4727922/publications.pdf Version: 2024-02-01



CAOHONC HE

#	Article	IF	CITATIONS
1	A Soluble and Highly Conductive Ionomer for Highâ€Performance Hydroxide Exchange Membrane Fuel Cells. Angewandte Chemie - International Edition, 2009, 48, 6499-6502.	13.8	541
2	Progress and prospects of next-generation redox flow batteries. Energy Storage Materials, 2018, 15, 324-350.	18.0	239
3	Quaternized poly(ether ether ketone) hydroxide exchange membranes for fuel cells. Journal of Membrane Science, 2011, 375, 204-211.	8.2	115
4	Highly Conducting Anion-Exchange Membranes Based on Cross-Linked Poly(norbornene): Ring Opening Metathesis Polymerization. ACS Applied Energy Materials, 2019, 2, 2458-2468.	5.1	109
5	Imidazolium-functionalized polysulfone hydroxide exchange membranes for potential applications in alkaline membrane direct alcohol fuel cells. International Journal of Hydrogen Energy, 2012, 37, 5216-5224.	7.1	102
6	Novel Triple Tertiary Amine Polymer-Based Hydrogen Bond Network Inducing Highly Efficient Proton-Conducting Channels of Amphoteric Membranes for High-Performance Vanadium Redox Flow Battery. ACS Applied Materials & Interfaces, 2019, 11, 5003-5014.	8.0	91
7	Construction of atomically dispersed Cu-N4 sites via engineered coordination environment for high-efficient CO2 electroreduction. Chemical Engineering Journal, 2021, 407, 126842.	12.7	91
8	A graphite intercalation compound associated with liquid Na–K towards ultra-stable and high-capacity alkali metal anodes. Energy and Environmental Science, 2019, 12, 1989-1998.	30.8	90
9	Design of pendent imidazolium side chain with flexible ether-containing spacer for alkaline anion exchange membrane. Journal of Membrane Science, 2017, 523, 216-224.	8.2	88
10	Polybenzimidazole membranes with nanophase-separated structure induced by non-ionic hydrophilic side chains for vanadium flow batteries. Journal of Materials Chemistry A, 2018, 6, 3895-3905.	10.3	88
11	Amphiprotic Side-Chain Functionalization Constructing Highly Proton/Vanadium-Selective Transport Channels for High-Performance Membranes in Vanadium Redox Flow Batteries. ACS Applied Materials & Interfaces, 2018, 10, 32247-32255.	8.0	80
12	Pulverizing Fe ₂ O ₃ Nanoparticles for Developing Fe ₃ C/Nâ€Codoped Carbon Nanoboxes with Multiple Polysulfide Anchoring and Converting Activity in Li‧ Batteries. Advanced Functional Materials, 2021, 31, 2011249.	14.9	79
13	A H ₃ PO ₄ preswelling strategy to enhance the proton conductivity of a H ₂ SO ₄ -doped polybenzimidazole membrane for vanadium flow batteries. RSC Advances, 2016, 6, 23479-23488.	3.6	78
14	Well-defined Fe–Cu diatomic sites for efficient catalysis of CO ₂ electroreduction. Journal of Materials Chemistry A, 2021, 9, 23817-23827.	10.3	77
15	Enhancement of hydroxide conductivity by the di-quaternization strategy for poly(ether ether ketone) based anion exchange membranes. Journal of Materials Chemistry A, 2014, 2, 12222.	10.3	71
16	Hydrophilic side chain assisting continuous ion-conducting channels for anion exchange membranes. Journal of Membrane Science, 2018, 552, 286-294.	8.2	71
17	Gradientâ€Distributed Metal–Organic Framework–Based Porous Membranes for Nonaqueous Redox Flow Batteries. Advanced Energy Materials, 2018, 8, 1802533.	19.5	70
18	A highly proton-conductive and vanadium-rejected long-side-chain sulfonated polybenzimidazole membrane for redox flow battery. Journal of Membrane Science, 2020, 596, 117616.	8.2	68

#	Article	IF	CITATIONS
19	Covalent organic framework (COF) constructed proton permselective membranes for acid supporting redox flow batteries. Chemical Engineering Journal, 2020, 399, 125833.	12.7	68
20	Quaternary phosphonium-functionalized poly(ether ether ketone) as highly conductive and alkali-stable hydroxide exchange membrane for fuel cells. Journal of Membrane Science, 2014, 466, 220-228.	8.2	63
21	Crosslinked poly (ether ether ketone) hydroxide exchange membranes with improved conductivity. Journal of Membrane Science, 2014, 459, 86-95.	8.2	59
22	An integrally thin skinned asymmetric architecture design for advanced anion exchange membranes for vanadium flow batteries. Journal of Materials Chemistry A, 2015, 3, 16948-16952.	10.3	59
23	Amphoteric-Side-Chain-Functionalized "Ether-Free―Poly(arylene piperidinium) Membrane for Advanced Redox Flow Battery. ACS Applied Materials & Interfaces, 2019, 11, 44315-44324.	8.0	58
24	Pendent piperidinium-functionalized blend anion exchange membrane for fuel cell application. International Journal of Hydrogen Energy, 2019, 44, 15482-15493.	7.1	58
25	Tri-quaternized poly (ether sulfone) anion exchange membranes with improved hydroxide conductivity. Journal of Membrane Science, 2016, 514, 613-621.	8.2	56
26	Guanidimidazole-quanternized and cross-linked alkaline polymer electrolyte membrane for fuel cell application. Journal of Membrane Science, 2016, 501, 100-108.	8.2	56
27	Thin skinned asymmetric polybenzimidazole membranes with readily tunable morphologies for high-performance vanadium flow batteries. RSC Advances, 2017, 7, 1852-1862.	3.6	50
28	"Fishnet-like―ion-selective nanochannels in advanced membranes for flow batteries. Journal of Materials Chemistry A, 2019, 7, 21112-21119.	10.3	50
29	Proton delivery through a dynamic 3D H-bond network constructed from dense hydroxyls for advanced ion-selective membranes. Journal of Materials Chemistry A, 2019, 7, 15137-15144.	10.3	50
30	Branched, Side-Chain Grafted Polyarylpiperidine Anion Exchange Membranes for Fuel Cell Application. ACS Applied Energy Materials, 2021, 4, 6957-6967.	5.1	50
31	Poly(2,6-dimethyl-1,4-phenylene oxide) containing imidazolium-terminated long side chains as hydroxide exchange membranes with improved conductivity. Journal of Membrane Science, 2016, 518, 159-167.	8.2	48
32	Dimensionally stable hexamethylenetetramine functionalized polysulfone anion exchange membranes. Journal of Materials Chemistry A, 2017, 5, 15038-15047.	10.3	47
33	Scalable High-Areal-Capacity Li–S Batteries Enabled by Sandwich-Structured Hierarchically Porous Membranes with Intrinsic Polysulfide Adsorption. Nano Letters, 2020, 20, 6922-6929.	9.1	47
34	Ultra-thin quaternized polybenzimidazole anion exchange membranes with throughout OH ^{â^'} conducive highway networks for high-performance fuel cells. Journal of Materials Chemistry A, 2021, 9, 7522-7530.	10.3	47
35	Pre-removal of polybenzimidazole anion to improve flexibility of grafted quaternized side chains for high performance anion exchange membranes. Journal of Power Sources, 2020, 451, 227813.	7.8	45
36	Proton conductivity enhancement of SPEEK membrane through n-BuOH assisted self-organization. Journal of Membrane Science, 2015, 479, 46-54.	8.2	42

#	Article	IF	CITATIONS
37	Electrospinning fiberization of carbon nanotube hybrid sulfonated poly (ether ether ketone) ion conductive membranes for a vanadium redox flow battery. Journal of Membrane Science, 2019, 583, 93-102.	8.2	42
38	Redistributing Li-ion flux and homogenizing Li-metal growth by N-doped hierarchically porous membranes for dendrite-free Lithium metal batteries. Energy Storage Materials, 2021, 37, 233-242.	18.0	41
39	Understanding of imidazolium group hydration and polymer structure for hydroxide anion conduction in hydrated imidazolium-g-PPO membrane by molecular dynamics simulations. Chemical Engineering Science, 2018, 192, 1167-1176.	3.8	40
40	The synergistic effect of protonated imidazole-hydroxyl-quaternary ammonium on improving performances of anion exchange membrane assembled flow batteries. Journal of Membrane Science, 2020, 603, 118011.	8.2	39
41	Patterned macroporous Fe ₃ C/C membrane-induced high ionic conductivity for integrated Li–sulfur battery cathodes. Journal of Materials Chemistry A, 2019, 7, 20614-20623.	10.3	37
42	Ion/Molecule-selective transport nanochannels of membranes for redox flow batteries. Energy Storage Materials, 2021, 34, 648-668.	18.0	37
43	High-Performance Anion Exchange Membranes with Para-Type Cations on Electron-Withdrawing Câ•O Links Free Backbone. Macromolecules, 2020, 53, 10988-10997.	4.8	36
44	Thermoplastic interpenetrating polymer networks based on polybenzimidazole and poly (1,) Tj ETQqO O O rgBT /(Overlock 1	0 Tf 50 462 1
45	Blend anion exchange membranes containing polymer of intrinsic microporosity for fuel cell application. Journal of Membrane Science, 2020, 595, 117541.	8.2	32
46	Highly Efficient Polysulfide Trapping and Ion Transferring within a Hierarchical Porous Membrane Interlayer for High-Energy Lithium–Sulfur Batteries. ACS Applied Energy Materials, 2020, 3, 5050-5057.	5.1	32
47	Electrospun nanofiber enhanced imidazolium-functionalized polysulfone composite anion exchange membranes. RSC Advances, 2015, 5, 95118-95125.	3.6	30
48	Molecular dynamics simulation on the effect of water uptake on hydrogen bond network for OHâ^' conduction in imidazolium-g-PPO membrane. International Journal of Hydrogen Energy, 2019, 44, 3760-3770.	7.1	30
49	One-step rapid synthesis of single thymine-templated fluorescent copper nanoclusters for "turn on― detection of Mn ²⁺ . Analytical Methods, 2017, 9, 2590-2595.	2.7	29
50	Electrochemical Reduction of CO ₂ in Proton Exchange Membrane Reactor: The Function of Buffer Layer. Industrial & Engineering Chemistry Research, 2017, 56, 10242-10250.	3.7	29
51	Anion exchange membranes with "rigid-side-chain" symmetric piperazinium structures for fuel cell exceeding 1.2†W†cmâ 2 at 60 ŰC. Journal of Power Sources, 2019, 438, 227021.	7.8	29
52	Friedel-Crafts alkylation route for preparation of pendent side chain imidazolium-functionalized polysulfone anion exchange membranes for fuel cells. Journal of Membrane Science, 2019, 573, 157-166.	8.2	29

53	Polybenzimidazole Ultrathin Anion Exchange Membrane with Comb-Shape Amphiphilic Microphase Networks for a High-Performance Fuel Cell. ACS Applied Materials & Interfaces, 2021, 13, 49840-49849.	8.0	29	
- 4	Paper-based visual detection of silver ions and <scp>l</scp> -cysteine with a dual-emissive nanosystem		0.0	

⁵⁴ of carbon quantum dots and gold nanoclusters. Analytical Methods, 2018, 10, 3945-3950. 2.7 28

#	Article	IF	CITATIONS
55	A novel membrane distillation response technology for nucleation detection, metastable zone width measurement and analysis. Chemical Engineering Science, 2015, 134, 671-680.	3.8	27
56	Modification of hydrophilic channels in Nafion membranes by DMBA: Mechanism and effects on proton conductivity. Journal of Polymer Science, Part B: Polymer Physics, 2014, 52, 1107-1117.	2.1	26
57	One-pot synthesis of enhanced fluorescent copper nanoclusters encapsulated in metal–organic frameworks. RSC Advances, 2018, 8, 22748-22754.	3.6	26
58	Hydrophilic/hydrophobic-bi-comb-shaped amphoteric membrane for vanadium redox flow battery. Journal of Membrane Science, 2020, 608, 118179.	8.2	26
59	Two-dimensional MoS2 nanosheets constructing highly ion-selective composite membrane for vanadium redox flow battery. Journal of Membrane Science, 2021, 623, 119051.	8.2	25
60	Ion conductive mechanisms and redox flow battery applications of polybenzimidazole-based membranes. Energy Storage Materials, 2022, 45, 595-617.	18.0	25
61	Hierarchically porous membranes for lithium rechargeable batteries: Recent progress and opportunities. EcoMat, 2022, 4, .	11.9	24
62	Oxygen vacancy enabled fabrication of dual-atom Mn/Co catalysts for high-performance lithium–sulfur batteries. Journal of Materials Chemistry A, 2022, 10, 11702-11711.	10.3	24
63	Improvement of alkaline stability for hydroxide exchange membranes by the interactions between strongly polar nitrile groups and functional cations. Journal of Membrane Science, 2017, 533, 121-129.	8.2	23
64	Hybrid anion exchange membrane of hydroxyl-modified polysulfone incorporating guanidinium-functionalized graphene oxide. Ionics, 2017, 23, 3085-3096.	2.4	22
65	Electron-Donating C-NH ₂ Link Backbone for Highly Alkaline and Mechanical Stable Anion Exchange Membranes. ACS Applied Materials & Interfaces, 2021, 13, 10490-10499.	8.0	22
66	One-step extraction of highly fluorescent carbon quantum dots by a physical method from carbon black. New Journal of Chemistry, 2017, 41, 5267-5270.	2.8	21
67	Hybrid Control Mechanism of Crystal Morphology Modification for Ternary Solution Treatment via Membrane Assisted Crystallization. Crystal Growth and Design, 2018, 18, 934-943.	3.0	21
68	Fluorescent carbon dots directly derived from polyethyleneimine and their application for the detection of Co ²⁺ . Analytical Methods, 2018, 10, 2989-2993.	2.7	21
69	One-pot synthesis of highly fluorescent Fe ²⁺ -doped carbon dots for a dual-emissive nanohybrid for the detection of zinc ions and histidine. New Journal of Chemistry, 2018, 42, 13651-13659.	2.8	21
70	Bis(oxazoline)-derived N-heterocyclic carbene ligated rare-earth metal complexes: synthesis, structure, and polymerization performance. Dalton Transactions, 2018, 47, 13815-13823.	3.3	21
71	Recent Advances in Rare Earth Complexes Containing N-Heterocyclic Carbenes: Synthesis, Reactivity, and Applications in Polymerization. Catalysts, 2020, 10, 71.	3.5	21
72	Imidazolium functionalized polysulfone electrolyte membranes with varied chain structures: a comparative study. RSC Advances, 2016, 6, 31336-31346.	3.6	20

#	Article	IF	CITATIONS
73	Side chain hydrolysis method to prepare nanoporous membranes for vanadium flow battery application. Journal of Membrane Science, 2018, 560, 67-76.	8.2	20
74	Structural contribution of cationic groups to water sorption in anion exchange membranes: A combined DFT and MD simulation study. Chemical Engineering Science, 2021, 244, 116791.	3.8	20
75	N-Doped Hierarchically Porous CNT@C Membranes for Accelerating Polysulfide Redox Conversion for High-Energy Lithium–Sulfur Batteries. ACS Applied Materials & Interfaces, 2021, 13, 2521-2529.	8.0	20
76	Low boiling point solvent-soluble, highly conductive and stable poly (ether phenylene piperidinium) anion exchange membrane. Journal of Membrane Science, 2022, 644, 120185.	8.2	20
77	Hollow COF Selective Layer Based Flexible Composite Membranes Constructed by an Integrated "Castingâ€Precipitationâ€Evaporation―Strategy. Advanced Functional Materials, 2022, 32, .	14.9	20
78	Construction of hierarchical proton sieving-conductive channels in sulfated UIO-66 grafted polybenzimidazole ion conductive membrane for vanadium redox flow battery. Journal of Power Sources, 2022, 526, 231132.	7.8	19
79	Anilido-oxazoline-ligated rare-earth metal complexes: synthesis, characterization and highly <i>ci</i> s-1,4-selective polymerization of isoprene. Dalton Transactions, 2019, 48, 3583-3592.	3.3	18
80	Epitaxial growth: rapid synthesis of highly permeable and selective zeolite-T membranes. Journal of Materials Chemistry A, 2017, 5, 17828-17832.	10.3	17
81	Facile and green fabrication of polybenzoxazine-based composite anion-exchange membranes with a self-cross-linked structure. Ionics, 2018, 24, 3053-3063.	2.4	16
82	Highly active rare-earth metal catalysts for heteroselective ring-opening polymerization of racemic lactide. Dalton Transactions, 2019, 48, 9079-9088.	3.3	14
83	Lutetium and yttrium complexes supported by an anilido-oxazoline ligand for polymerization of 1,3-conjugated dienes and ε-caprolactone. New Journal of Chemistry, 2020, 44, 121-128.	2.8	13
84	Synthesis of highly luminescent Cu/Ag bimetal nanoclusters and their application in a temperature sensor. Analytical Methods, 2017, 9, 4028-4032.	2.7	12
85	Poly (ether ether ketone ketone) based imidazolium as anion exchange membranes for alkaline fuel cells. Chinese Journal of Chemical Engineering, 2018, 26, 2130-2138.	3.5	12
86	Covalent/ionic co-crosslinking constructing ultra-densely functionalized ether-free poly(biphenylene) Tj ETQq0 0 359, 136879.	0 rgBT /C 5.2	verlock 10 Tf 12
87	Amphiphilic cone-shaped cationic calix[4]arene composite anion exchange membranes with continuous ionic channels. Journal of Membrane Science, 2021, 640, 119815.	8.2	12
88	Nanoscale Solid Superacid-Coupled Polybenzimidazole Membrane with High Ion Selectivity for Flow Batteries. ACS Sustainable Chemistry and Engineering, 2020, 8, 16493-16502.	6.7	11
89	Constructing ionic channels in anion exchange membrane via a Zn2+ soft template: Experiment and molecular dynamics simulation. Journal of Membrane Science, 2021, 629, 119293.	8.2	10
90	Membrane crystallization: Engineering the crystallization via microscale interfacial technology. Chemical Engineering Research and Design, 2022, 178, 454-465.	5.6	10

#	Article	IF	CITATIONS
91	RCB-multicolor fluorescent carbon dots by changing the reaction solvent type for white light-emitting diodes. New Journal of Chemistry, 2022, 46, 4979-4982.	2.8	10
92	Improving CO ₂ Electroreduction Activity by Creating an Oxygen Vacancy-Rich Surface with One-Dimensional In–SnO ₂ Hollow Nanofiber Architecture. Industrial & Engineering Chemistry Research, 2021, 60, 1164-1174.	3.7	9
93	Micro-phase separation promoted by electrostatic field in electrospinning of alkaline polymer electrolytes: DFT and MD simulations. Chemical Engineering Science, 2022, 248, 117171.	3.8	9
94	Formation Mechanism of the Spiral-Like Structure of a Hydrogen Bond Network Confined in a Fluorinated Nanochannel: A Molecular Dynamics Simulation. Journal of Physical Chemistry C, 2017, 121, 13840-13847.	3.1	8
95	Anion exchange membrane with well-ordered arrays of ionic channels based on a porous anodic aluminium oxide template. Journal of Applied Electrochemistry, 2018, 48, 1151-1161.	2.9	7
96	Tailored 3D printed micro-crystallization chip for versatile and high-efficiency droplet evaporative crystallization. Lab on A Chip, 2019, 19, 767-777.	6.0	7
97	Enabling high Anion-selective conductivity in membrane for High-performance neutral organic based aqueous redox flow battery by microstructure design. Chemical Engineering Journal, 2022, 432, 134268.	12.7	7
98	Engineering amino-mediated copper nanoclusters with dual emission and assembly-to-monodispersion switching by pH-triggered surface modulation. New Journal of Chemistry, 2021, 45, 13262-13265.	2.8	6
99	Nanocage-oriented induction for highly ion-selective sub-1-nanometer channels of membranes. Journal of Materials Chemistry A, O, , .	10.3	5
100	Coordination Polymerization of α,ï‰-Dienes Using Single-Site Metal Catalysts. Mini-Reviews in Organic Chemistry, 2016, 13, 349-362.	1.3	3
101	Red fluorescent carbon dots excited by visible light: cell imaging and visual detection of ammonia gas using PVB films. New Journal of Chemistry, 2021, 45, 22869-22875.	2.8	2
102	Facile fabrication of titanosilicate zeolites with an unprecedented wide range of Si/Ti ratios by employing transition metal dichalcogenides as metal precursors. CrystEngComm, 2020, 22, 164-168.	2.6	1